



**HAL**  
open science

# The use of pith in the formulation of lightweight bio-based composites: Impact on mechanical and hygrothermal properties

Mohamed Said Abbas, Fionn Mcgregor, Antonin Fabbri, Mohammed Yacine Ferroukhi

## ► To cite this version:

Mohamed Said Abbas, Fionn Mcgregor, Antonin Fabbri, Mohammed Yacine Ferroukhi. The use of pith in the formulation of lightweight bio-based composites: Impact on mechanical and hygrothermal properties. *Construction and Building Materials*, 2020, 259, pp.120573. 10.1016/j.conbuildmat.2020.120573 . hal-03011243

**HAL Id: hal-03011243**

**<https://hal.science/hal-03011243>**

Submitted on 5 Sep 2022

**HAL** is a multi-disciplinary open access archive for the deposit and dissemination of scientific research documents, whether they are published or not. The documents may come from teaching and research institutions in France or abroad, or from public or private research centers.

L'archive ouverte pluridisciplinaire **HAL**, est destinée au dépôt et à la diffusion de documents scientifiques de niveau recherche, publiés ou non, émanant des établissements d'enseignement et de recherche français ou étrangers, des laboratoires publics ou privés.



Distributed under a Creative Commons Attribution - NonCommercial 4.0 International License



1 630 kg/m<sup>3</sup>. The same range of values was measured by [11][12][13] for hemp composites made with  
2 lime and metakaolin and by [14] for maize and sunflower stalk based composites. In all these cases,  
3 the sample densities were ranging between 500 and 600 kg/m<sup>3</sup>. [15] studied the impact on thermal  
4 conductivity of the composition of two corn stalk and magnesium phosphate cement composites.  
5 They noticed that samples with a higher corn stalk content had a lower thermal conductivity. [16]  
6 found this same result on hemp composites, detailing however that the relation between the  
7 amount of hemp shiv and thermal conductivity is not linear. Furthermore, [15] observed that for a  
8 same corn stalk content, large stalks presented a lower thermal conductivity than small ones, which  
9 was explained by a lower density and a higher porosity. Many parameters have an impact on thermal  
10 properties of bio-based composites such as water content, density and the formulation. It has been  
11 highlighted in the past that density has the biggest influence because a larger air volume in the  
12 material results in a low thermal conductivity [10][15][16].

13 In addition to their promising thermal performances, bio-based composites are known to exhibit  
14 good to excellent hygroscopic potential [9][17]. It traduces their ability to be used as a passive  
15 humidity regulation system thanks to their high capacity of adsorption (and desorption) of water  
16 vapor molecules from (to) the surrounding atmosphere. Due to the latent heat of adsorption and  
17 desorption processes, these materials might also have the potential to be used as passive  
18 temperature regulation system [11], even if the real impact of this effect on building energy  
19 consumption still needs to be better assessed.

20 Other important assets of bio-based composites are their high vapor permeancy and their light  
21 weight, which make them suitable to be used to rehabilitate the national heritage, typically built in  
22 stone, adobe, rammed-earth, etc. [14][16][18]. Indeed, they do not constrict vapor exchanges  
23 between walls and their environment and they do not overcharge the existing structure.

24 On the other side, bio-based composites do not have mechanical performances as good as classic  
25 building materials [10][17][19][20]. That is why they are most of the time rather used as filling and/or  
26 insulation materials, for which a high loading capacity is not mandatory. Anyway, it is commonly  
27 agreed that compressive strength and deformation modulus are good indicators of binder-aggregate  
28 compatibility. The several studies led on these parameters lead to the conclusion that there is no  
29 good or bad aggregate or binder, but good or bad combinations of them [21]. For example, [22] show  
30 that a first composite made of corn stalk and ordinary Portland cement threw a 1.5 MPa compressive  
31 strength value, while a second composite made of corn stalk and magnesium phosphate cement  
32 presented a compressive strength more than two times higher (3.83 MPa). Another sound example is  
33 given by [14]. In this study compressive strength at 60 days was measured on composites made of  
34 lime and sunflower (LS) with a density of 540 kg/m<sup>3</sup>, metakaolin and sunflower (MS) with a density of  
35 510 kg/m<sup>3</sup> and finally, metakaolin and maize bark (MM) with a density of 530 kg/m<sup>3</sup>. These  
36 composites developed a mechanical resistance of 0.21 MPa, 0.34 MPa and over 0.35 MPa  
37 respectively.

38 Most of the time, the aggregate used in the formulation of bio-based composites is the hemp shiv. In  
39 France, for example, the soles professional rules that exist for this kind of materials are dedicated to  
40 hemp composite [5]. Nonetheless, it is essential to give alternatives to hemp [8][14][23] so as to have  
41 access to varied resources regarding geographical origin with the goal of reducing transport carbon  
42 print. For that purpose, a large variety of aggregates can be found, such as flax, straw, wood, coconut,  
43 miscanthus, corn or sunflower, etc. [18][19][24][25][26].

1 Based on this observation, this paper focuses on sunflower and maize pith, which, like hemp shiv, are  
2 considered as agricultural by-products. Both sunflower and maize grow in most European countries  
3 and they already have been studied by some authors [14][23][27][28][29][30][31].

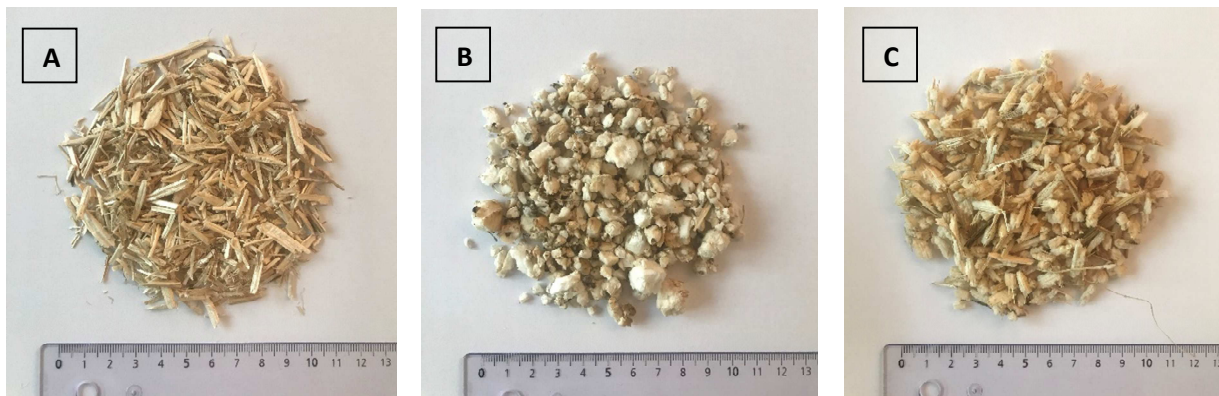
4 The binders used are lime based and contain cement and admixtures in certain cases. The goal is to  
5 determine the impact of the use of pith instead of hemp on the performance of the composite. For  
6 that purpose, two ranges of densities (low densities around  $150 \text{ kg/m}^3$  and medium densities around  
7  $500 \text{ kg/m}^3$ ) and three binders are considered. Let us underline that it has already been determined in  
8 a previous paper [32] that the geographical origin of the sunflower and maize piths does not impact  
9 the performance of the composites. Their performance was assessed through their mechanical,  
10 thermal, sorption and vapor transport properties. Thermal conductivity was studied through two  
11 different methods, the hot wire method and a novel device conceived for more accurate  
12 measurement. Finally, the hygrothermal potentials of the composites were evaluated through the  
13 moisture buffering test, and the consistency between results was analyzed using the MBV analytical  
14 expression provided by [33].

15 Since hemp dominates the bio-based construction field and the regulations about vegetal composites  
16 are based on it, the aim of this paper is to determine whether maize and sunflower pith aggregates  
17 can be used at the same level, not to replace hemp but to provide more choice. In addition, the  
18 impact of the aggregate, of the binder and of the interaction of both will be assessed. We will as well  
19 determine whether used binders, which have originally been conceived for hemp shiv, are  
20 appropriate for maize and sunflower pith or not.

## 21 2. Materials

### 22 2.1 Plant aggregates

23 As part of this experimental campaign, three types of plant aggregates were studied: hemp shiv (H),  
24 sunflower pith (S) and maize pith (M) (cf. **Fig 1**). The hemp shiv aggregates were received from an  
25 agriculture cooperative based in the north of France. Loose hemp shiv aggregates had a density of  
26  $100 \text{ kg/m}^3$ , an average width of 4.1 mm and an average length of 7.6 mm. The sunflower pith comes  
27 from an agriculture cooperative based in the south-east of France. Loose density of this sunflower  
28 pith was around  $14 \text{ kg/m}^3$ , an average diameter of the aggregates was around 4.2 mm. The maize  
29 pith comes from an agriculture cooperative based in west France with a more oceanic climate. The  
30 maize pith aggregates had a loose density of  $18 \text{ kg/m}^3$ , an average width of 2.2 mm and an average  
31 length of 9.6 mm. The density of the aggregates has been determined following [34]'s protocol,  
32 whereas the average aggregate dimensions have been calculated through a sifting granulometric  
33 curve for pith and through a 2D image granulometric analysis developed by [35] for hemp shiv.



34 **Fig. 1.** Aggregates used in this study (A) Hemp shiv, (B) Sunflower pith and (C) Maize pith

1 **2.2 Binders**

2 Three different types of binders were used in this study. The first one named C1 is a calcic lime based  
 3 binder. The second one named C2, is a formulated lime which is composed of hydraulic lime,  
 4 calcareous charges, hydrophobic and rheological admixtures. The last one, named HB, is a cement  
 5 and lime mixture with further additives, this formulation was developed by an industrial partner and  
 6 whose exact composition is not available.

7 **2.3 Bio-based composites**

8 The samples were manufactured in the same conditions (50%RH and 23°C) and the main proportion  
 9 of the mixtures of all kinds of formulations used are summarized in **Table 1**. Samples were sprayed in  
 10 cylindrical formworks with a 16 cm diameter and a 32 cm height in a single layer except for C2-H\*,  
 11 which was manufactured in 6 layers of about 5 cm each. Each layer was compacted at 0.05 MPa  
 12 following [5]. It is recalled that H, S and M are the aggregates explained in §2.1, more specifically  
 13 hemp shiv, sunflower pith and maize pith respectively, while C1, C2 and HB are the binders explained  
 14 in §2.2. C2-H\* corresponds to a formulation that was compacted.

15  
 16  
 17 **Table 1** Summary of the formulation and mass ratio.

Type of binder	C1	C2				HB		
Type of aggregates	H	H	H*	S	H+S	H	S	M
Designation	C1-H	C2-H	C2-H*	C2-S	C2-H+S	HB-H	HB-S	HB-M
Hemp shiv/binder** (-)	0.33	0.33	0.33	0	0.17	0.33	0	0
Pith/binder** (-)	0	0	0	0.10	0.06	0	0.20	0.16
Water/binder** (-)	0.81	0.88	0.88	0.80	1.07	0.88	2.92	2.92
Mass proportion of hemp shiv (-)	0.15	0.15	0.15	0	0.07	0.15	0	0
Mass proportion of pith (-)	0	0	0	0.05	0.03	0	0.05	0.04

18 \* corresponds to a formulation which has been densified using a tamper tool.

19 \*\* correspond to mass ratio between constituents

20 A pycnometer was used in order to determine the physical properties such as the skeletal porosity,  
 21 dry and skeletal densities of the different formulations according to the standard NF EN 1097-7 2008.  
 22 Results are shown in the **Table 2**.

23 **Table 2** Summary of the physical characteristics.

Formula tion	C1-H	C2-H	C2-H*	C2-S	C2-H+S	HB-H	HB-S	HB-M
Porosity	0.76±0.0	0.79±0.0	0.70±0.0	0.77±0.0	0.70±0.0	0.78±0.0	0.94±0.0	0.92±0.0
	2	1	2	1	2	2	1	1
Dry density (kg/m <sup>3</sup> )	470 ±5	440 ±6	600 ±10	550 ±5	590 ±6	410 ±8	150 ±4	160 ±5

Skeletal density (kg/m <sup>3</sup> )	1960	2090	2000	2390	1970	1860	2500	2000
---------------------------------------	------	------	------	------	------	------	------	------

1

2 The formulations C2-H\*, C2-H+S and C2-S aimed at testing the impact of the aggregate on the  
 3 performance. Indeed, they were mixed with different aggregates but with the same binder, and their  
 4 dry densities are in the same range. The formulation C2-H, which is similar to C2-H\*, was made to  
 5 test the impact of a moderate variation of density.

6 The impact of the binder will be assessed through the comparative analysis of the results of the C1-H,  
 7 C2-H and HB-H formulations.

8 Finally, two light formulations, namely HB-S and HB-M were made in order to test the ability of pith  
 9 aggregate to be used in light composites with high thermal performances. **Fig. 2A and 2B** show a HB-  
 10 S and a C1-H specimen respectively.

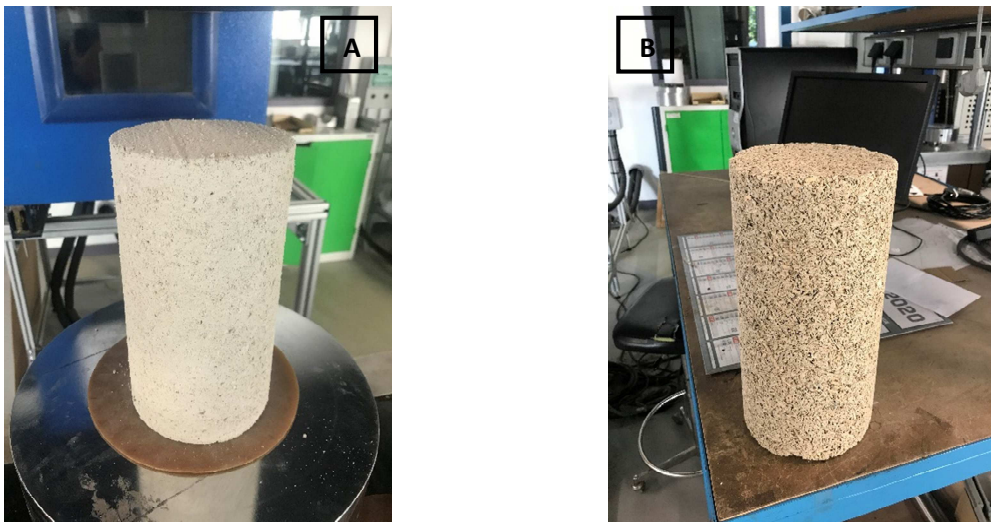


**Fig. 2.** A 16\*32 cm HB-S specimen (A) and a 16\*32 cm C1-H specimen (B)

11

12 **2.4 Methods**

13 **2.4.1. Uniaxial compression test**

14 To study the mechanical properties of materials, non-cyclic uniaxial compression tests were  
 15 performed as done by [18][36][37][38] in accordance with French professional rules “Building with  
 16 hemp”. Both compressive strength (Rc) and global initial deformation modulus were evaluated. For  
 17 each value, three uniaxial compression tests have been performed.

18 Compressive strength increases gradually during the hydration process. [18] studied a series of  
 19 composites made of a mixture of hydraulic and air lime, hemp and water in which each composite  
 20 had a different binder percentage and she observed a common pattern. All the composites  
 21 presented three phases of strength development, the first between 0 and 3 months, in which  
 22 compressive strength doubled its value; the second one between 3 months and 1 year, when  
 23 compressive strength increased by 10 to 50% depending on the formulation, and a third one after  
 24 one year, in which Rc increased by 10% every year.

1 To study this strong temporal evolution during the first 3 months, uniaxial compression tests were  
2 made at two curing times (28 and 60 days). Some tests were performed after a curing of 90 days, but  
3 the results were not presented here since they were found to be similar to those at 60 days.

4 Mechanical strength and deformation modulus were determined on the “dense formulations” HB-H,  
5 C2-H+S and C2-S and the “light formulations” HB-M and HB-S. The tests were carried out on  
6 cylindrical samples of 16\*32 cm using an INSTRON press controlled at 3 mm/min displacement.

7 Before the compression tests, samples were stored at  $23 \pm 2^\circ\text{C}$  and 50%RH, then dried in an oven at  
8  $50 \pm 1^\circ\text{C}$  for 96 hours following the [5] recommendations. The tests were performed in triplicate, and  
9 the average reading was reported. Density of each sample was measured before testing.

#### 10 **2.4.2. Thermal conductivity**

11 Two techniques were used in order to measure the thermal conductivity.

12 The hot wire apparatus was used for all the formulations. For that purpose, cylindrical specimens  
13 16\*32 cm of composite were cut after 21 days of manufacture in small cylindrical samples (16\*6 cm),  
14 which allowed us to obtain three samples per formulation. They were conserved in a room at about  
15  $30^\circ\text{C}$  ( $\pm 5^\circ\text{C}$ ) and 60%RH ( $\pm 5\%$  RH) and were tested after 100 days of curing. In these same conditions,  
16 the thermal conductivity measurement of the plant aggregates was carried out using plastic boxes  
17 filled with hemp shiv (H) and sunflower pith (S), following the procedure presented in [9]. Each  
18 formulation was tested using the three different samples, the results being the arithmetic mean  
19 value of the three tests.

20 The hot wire method is however frequently pointed out due to some of its limitations. Namely that  
21 the area covered by the probe which emits heat is fairly representative, and that the samples have  
22 irregularities on the surface, which makes the heat transfer not unidirectional.

23 To avoid these issues and to check accuracy of the hot wire measurements, a novel measuring device  
24 has been developed. This device measures the thermal conductivity of a representative sample  
25 (35\*35\*7 cm). The principle is similar to the hot plate's, which consists in creating a unidirectional  
26 heat flow crossing the thickness of our sample by imposing a thermal gradient between two  
27 chambers, a cold one and a hot one. The chambers (A and B) are made of wood and configured as  
28 seen in the **Fig. 3**, the warm atmosphere being monitored by a PID controller (Proportional Integral  
29 Derivative) and the heat being generated using a light bulb. The cold atmosphere is generated by a  
30 cryostat. Both the PID and the cryostat are connected to a computer. In order to homogenize, the  
31 atmosphere is ventilated in the two compartments.



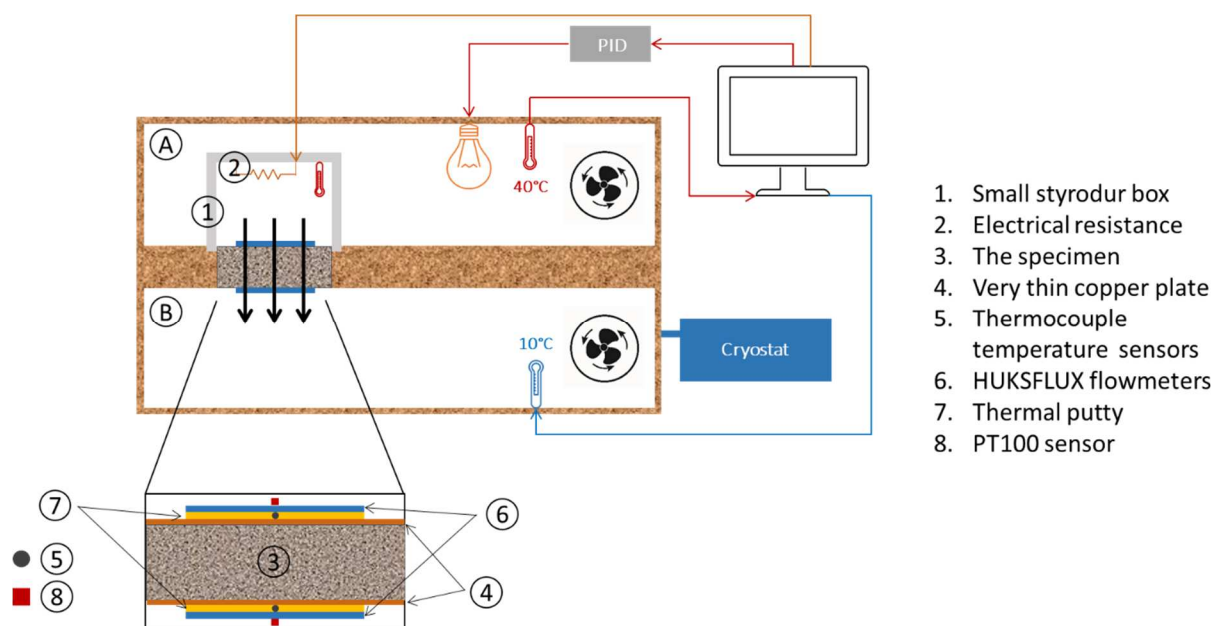


**Fig. 3.** Thermal conductivity measuring device.

A small styrodur box (1) has been manufactured and placed above the sample in such a way that there is no heat loss to the outside environment. Without it, the hot environment around the sample would suffer heat leaks and would not be stable. This box is heated using an electrical resistance (2) controlled by a computer. A temperature sensor has been placed in each compartment. The sample (3) is placed in the cavity that connects both chambers. Once the sample is placed, we stick on both sides a very thin copper plate (4), which has a very high thermal conductivity, in order to ensure a flat surface that guarantees a unidirectional vertical thermal field. On the latter, thermocouple temperature sensors (5) are taped with aluminum tape to keep track of the temperature during the test. We then glue the HUKSFLUX flowmeters (6) using thermal putty (7) to ensure good thermal conductivity and on top of that, we add another PT100 sensor (8) to measure the value of the surface temperature. The device has been calibrated using polystyrene, whose thermal conductivity is well known. This test was performed on three formulations, HB-S, C1-H and HB-H, and for each of them, three samples were studied. The results in § 3.2 are the arithmetic average for each formulation. In the sake of comparability, samples were stored at the same conditions as hot wire's, 30°C ( $\pm 5^\circ\text{C}$ ) and 60%RH ( $\pm 5\%RH$ ), and tested after 100 days of curing. This age was chosen because the variation of mass was under 1% between two measures performed 24 hours apart. For the test, the temperature difference was established at 30°C, with 40°C in the hot atmosphere (both outside and inside the styrodur box to ensure a stable temperature) and 10°C in the cold one. This values can be configured by the user. Humidity conditions have no impact since the sample is completely covered by the copper plates on both faces and surrounded by aluminum scotch.

This device has been dimensioned to perform tests as long as the user requires, but in this experimental campaign, the tests took approximately 30 minutes, the time to achieve the heat flux steady state through the sample.

### 2.4.3. Sorption isotherms

Two methods were used for the determination of the sorption curves: "desiccator method" and "DVS method". The equivalence between these two methods has already been discussed in [39]. It requires that the protocols used to measure the dry masses in each method lead to the same dry density, which was here successfully checked.



1 The “desiccator method” was performed on three representative samples of formulations HB-H, HB-  
2 S, HB-M, C2-H and C1-H according to the standard EN ISO 12571 (CEN 2000). The samples were cubic  
3 and had 4 cm in edge. This representative volume was determined from the apparent density  
4 variation against volume [40]. The first step was to dry all samples in an oven at 50°C in order to start  
5 the test at dry mass. Since the samples contained organic material, the maximum temperature that  
6 could be used was 60°C, because the fibers in the material may suffer from degradation at higher  
7 temperatures. To ensure the reproducibility of dry mass measurements and the consistency between  
8 desiccator and DVS methods, the relative humidity within the oven was checked to be lower than 5%.  
9 The samples were placed in six different levels of RH (23, 43, 59, 75 and 85%) using saline solutions.  
10 For this test, the temperature was maintained at 23±2°C. A portable sensor (Rotronic HygroLog HL-  
11 NT) was used for constant control of the RH and the temperature in the boxes. The starting point of  
12 the sorption curve corresponds to the dry mass of the samples. After finding the initial point of the  
13 curve, the samples are then placed at relative humidity values aforementioned following an  
14 adsorption stage and then a desorption stage.  
15 The Dynamic Vapor System (DVS Intrinsic SMS) method was used to draw the sorption curves of the  
16 aggregates H, M and S and of the formulations HB-M, HB-S, C2-S, C2-H+S and C2-H\*. For both  
17 methods, each formulation was tested using three samples and the given results are the arithmetic  
18 average of the three samples of each formulation. HB-M and HB-S were tested using both methods in  
19 order to check if results were close. Since they were, the values shown in §3.3 for these two  
20 formulations are only those obtained through the DVS.

21

#### 22 **2.4.4. Water vapor permeability (Wet Cup method)**

23 The water vapor permeability of all formulations was measured using the Wet Cup method according  
24 to the standard EN ISO-12572 (CEN 2001). It consists in generating a vapor pressure gradient by  
25 adjusting the relative humidity to 50% in the climatic chamber and 85% in the cup. The space  
26 between the saline solution and the bottom of the sample is called the air layer and was 20mm for all  
27 samples. The set-up of the cups was performed according to the procedure followed by [41].  
28 Therefore, a thin layer of silicone was applied to seal the samples on Plexiglas cups. A vapor-tight  
29 aluminum tape was used to seal the sides of the sample with the side of the cup. The use of  
30 aluminum tape is justified by its properties: it is impervious and does not absorb moisture itself [42].  
31 Environmental conditions (50% RH and 23°C) were constantly monitored by the climatic chamber.  
32 For each formulation, samples of 3 thicknesses (2 cm, 4 cm and 6 cm) were tested in order to take  
33 into account the surface resistance effect, as it was recommended by [43]. The result for the vapor  
34 permeability of each formulation is the arithmetic average of the value for each thickness. As  
35 explained by McGregor, the water vapor permeability value for each sample takes into account the  
36 effect of the sample’s thickness.

#### 37 **2.4.5. Dynamic moisture exchange behavior (Moisture Buffering Value)**

38 In order to quantify the hygroscopic potential of a porous medium, a common method consists in  
39 performing a dynamic adsorption-desorption test commonly called MBV. The protocol for this test  
40 was initially defined as part of the NordTest project. This test indicates the amount of moisture  
41 absorbed or released by a material when exposed to cycles of repeated relative humidity changes  
42 between 33% and 75% at 23°C, with time steps of 8 hours to high relative humidity and 16 hours  
43 durations at low relative humidity (other relative humidity cycles can be chosen, but in our case we  
44 have maintained reference cycle values) [33]. The tested sample is sealed on all sides using aluminum  
45 tape, except for the upper side, and the Practical Moisture Buffering Value is calculated as the mass  
46 variation per unit area (denoted  $A$ ) according to the formula:

47

$$MBV_{\text{practical}} = \frac{\Delta m}{A * \Delta RH} \quad (1)$$

with  $\Delta m$  (in g) the mass variation during the cycle,  $\Delta RH$  the variation of relative humidity (in %) and  $MBV_{\text{practical}}$  the Practical Moisture Buffering Value expressed in  $g/(m^2\%RH)$ .

Cylindrical specimens 16\*32 cm were cut beforehand to make 3 identical samples of size 16\*6cm for each type of insulation, which makes us a total of 27 samples. The result for each formulation is the arithmetic mean of the three samples. The mass monitoring was carried out with an interval of 1 hour then 2 hours until reaching the maximum of the cycle and then a last measurement 24h after the beginning of the cycle. The MBV was calculated when the regime was stabilized, i.e. when the mass difference between the beginning and the end of a cycle was less than 5%.

### 3. Results

#### 3.1. Uniaxial compression test

The results of the uniaxial compression test are reported in the **Table 3**. The apparent global deformation modulus (E) was estimated on the linear part of the axial stress-axial strain curve. The compression resistance  $R_c$  is considered to be the limit between the elastic and elasto-plastic behavior of the axial stress – axial strain curve, which happened at  $3\% \pm 0.5$  strain in all cases. The apparent global stiffness modulus (E) is estimated as the slope of the linear part of the curve. As bio-based composites typically present a heterogeneous deformation, strain has been determined as the variation of the total thickness of the sample divided by the initial thickness using a position sensor incorporated in the press.

**Table 3** Average of global stiffness modulus of the formulations.

Type of samples	HB-H	HB-S	HB-M	C2-H+S	C2-S
Density (kg/m <sup>3</sup> )	410 ±8	150 ±4	160 ±5	590 ±6	550 ±5
Rc <sub>28</sub> (MPa)	0.53 ±0.03	0.10 ±0.01	0.11 ±0.02	0.58 ±0.03	0.50 ±0.01
E <sub>28</sub> (MPa)	46 ±2.1	-	-	52.6 ±2.7	50.5 ±1.2
Rc <sub>60</sub> (MPa)	0.66 ±0.02	0.27 ±0.01	0.24 ±0.03	0.78 ±0.02	0.64 ±0.02
E <sub>60</sub> (MPa)	68.5 ±1.8	10.0 ±0.8	7.5 ±1	73.8 ±2.4	64.5 ±1.6

Results of HB-S and HB-M appeared to be clearly different from the others (namely HB-H, C2-H+S and C2-S). Compressive strength values at 28 days of 0.10-0.11 MPa were found for HB-S and HB-M, and of 0.5-0.58 MPa for the other three. At 60 days, compressive strength increased up to 0.24-0.27 MPa for HB-S and HB-M, while the three others reached 0.64-0.78 MPa. The deformation modulus also appears to be strongly lower for HB-S and HB-M formulations, as well as the ratio between the deformation modulus and the compressive strength. For HB-H, C2-H+S and C2-S formulations,  $E_{60}/Rc_{60} \approx 100$  while  $E_{60}/Rc_{60} \approx 35$  for HB-S and HB-M. These significant differences in behavior can be explained by their dissimilar density (150-160 kg/m<sup>3</sup> for HB-S and HB-M while the others range from 410 to 590 kg/m<sup>3</sup>).

To go further in the analysis, the compressive strength values obtained at 28 days in this study were compared with the ones reported in literature for hemp, corn stalk and pith composites. Results are reported in **Fig. 4**.

At first, it can be seen that our values are in the range of ones reported in literature. In this graph, the strong impact of the dry density on the compressive strength, whatever binder and aggregate

1 natures appears to be quite obvious. However, a closer look seems to indicate that, for a given  
 2 density, compressive strength is slightly lower for pith-based composites than for hemp-based  
 3 composites. This tendency can be also observed in the results of this study from the comparison  
 4 between C2-S+H, C2-S and HB-H formulations. A possible explanation might be the higher porosity of  
 5 pith (see **Table 2**), which results in a low compressive strength of the aggregates. It is however quite  
 6 complicated to conclude on that point, since it is not possible to keep constant both dry density and  
 7 particle/binder ratio, and these two parameters are known to significantly impact both compressive  
 8 strength and deformation modulus. Thus, a precise assessment of the impact of aggregate nature on  
 9 the mechanical performance would have required a more extensive campaign of uniaxial  
 10 compression test, which was clearly out of the scope of this paper.

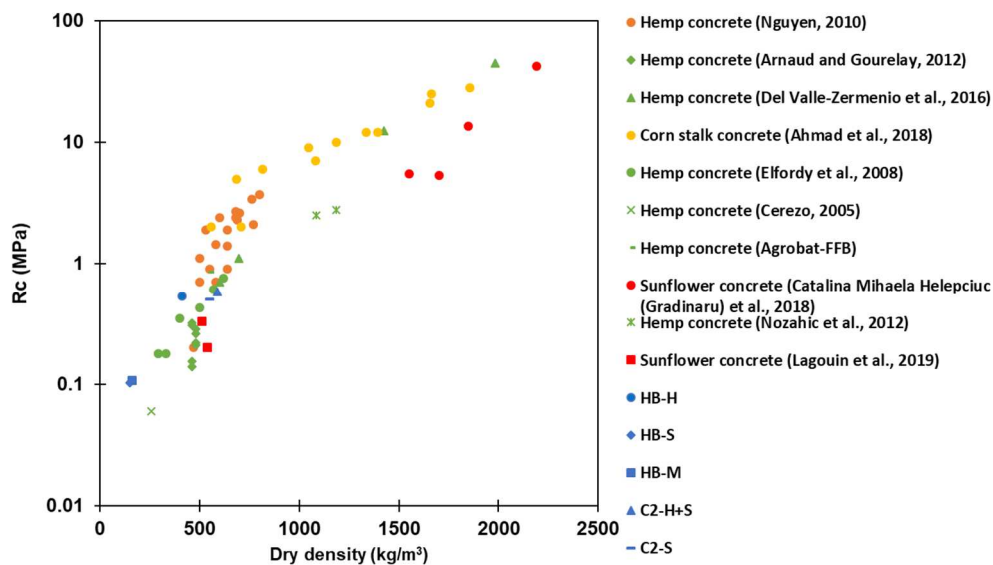


**Fig. 4.** Compressive strength vs dry density at 28 days of the formulations tested in this study and from several studies from literature

11  
 12 Anyway, we can conclude that all the formulations studied in this paper led to sufficiently cohesive  
 13 materials in order to be used for building insulation purposes. In the framework of the French hemp  
 14 construction guide “Building with hemp” specifications [5], HB-S and HB-M can be used only for roof  
 15 applications while HB-H, C2-H+S and C2-S can be used as a plaster, a wall, floor or roof. The other  
 16 main information is that the use of pith instead of hemp does not prejudicially drop the mechanical  
 17 performance of the composite, even if it might slightly reduce it.

18  
 19 **3.2. Thermal conductivity**

20 The results of thermal conductivity are shown in the **Table 4**.  $\lambda_{\text{hot wire}}$  represents the thermal  
 21 conductivity measured with the hot wire apparatus, while  $\lambda_{\text{new device}}$  is the one measured with the  
 22 home-made device presented in the §2.4.2.

**Table 4** Summary of the thermal parameters of the tested formations.

Type of samples	Density (kg/m³)	$\lambda_{\text{hot wire}}$ (mW/(m.K))	$\lambda_{\text{new device}}$ (mW/(m.K))
-----------------	-----------------	--	--

<b>C2-S</b>	550 ±5	190 ±7	-
<b>C2-H</b>	440 ±6	135 ±10	-
<b>C2-H*</b>	600 ±10	150 ±10	-
<b>C2-H+S</b>	590 ±6	140 ±8	-
<b>HB-S</b>	150 ±4	65 ±2	66 ±1
<b>HB-M</b>	160 ±5	75 ±3	-
<b>C1-H</b>	470 ±5	155 ±10	147 ±2
<b>HB-H</b>	410 ±8	90 ±10	75 ±2
<b>Hemp shiv (H)</b>	100 ±5	70 ±6	-
<b>Sunflower pith (S)</b>	14 ±4	50 ±1	-

1 Values obtained with the two methods are not strongly different but they show some inaccuracies.  
2 For HB-S it can be observed that both values are almost identical. However, results are not as good  
3 for C1-H and for HB-H, for which hot wire apparatus tends to higher values. The main difference  
4 between the specimens is that samples containing sunflower pith present a flat surface whereas  
5 hemp samples show strong irregularities on the surface. One reason of this trend could be that the  
6 size of the material heterogeneities (size of aggregates and pores) is too large for hemp-based  
7 formulations compared to the zone scanned by the hot wire. It leads to underestimate the thermal  
8 insulation contribution caused by the porosity of the material. However, the tendencies obtained  
9 with the hot wire were found to be correct and this method can be used for comparison purposes.

10 The first analysis that can be made is that the general tendency is a decrease of the thermal  
11 conductivity with density. This is consistent with observations made in previous studies, describing  
12 this tendency [14].

13 Thermal conductivity measurements were also made on loose aggregates. A thermal conductivity of  
14 0.07 W/(m.K) was found for Hemp shiv (H), while 0.05 W/(m.K) was found for sunflower pith (S).  
15 These results appeared to be a bit higher than expected, but the significantly lower thermal  
16 conductivity of sunflower pith when compared to hemp shiv was quite expected.

17 This tendency is however reversed once the aggregates are mixed with the binder. For example, the  
18 thermal conductivities of both C2-H and C2-H\* are lower than C2-S's one, even if they were  
19 formulated with the same binder and if their densities are in the same range (440 kg/m<sup>3</sup> for C2-H,  
20 600 kg/m<sup>3</sup> for C2-H\* and 550 kg/m<sup>3</sup> for C2-S). The same conclusion can arise from the comparison  
21 between HB-S and HB-H. While it exhibits a significantly higher dry density (410 kg/m<sup>3</sup> vs 150 kg/m<sup>3</sup>),  
22 the thermal conductivity of HB-H appears to be only slightly higher than those of HB-S (0.075 W/(m.K)  
23 vs 0.066 W/(m.K)). Therefore, thermal conductivity of the composite is found to be impacted by the  
24 type of aggregate. But this impact is not trivial. It can notably depend on the coating rate of the  
25 particle by the binder, as well as on the physical and/or chemical interactions between them. It will  
26 thus not be possible to predict easily the thermal conductivity of the composite from the knowledge  
27 of the thermal conductivities of its constituents. Let us underline that this result is in contradiction  
28 with [9], which found no significant influence of the nature of the aggregates on the thermal  
29 conductivity of bio-based composites. Additional studies are thus required in order to draw a  
30 definitive conclusion on that point.

31 Another analysis that can be made is the impact of the binder, for a given density and type of  
32 aggregate. No clear consensus exists on that point. While [9][44] mentioned that binder and, more  
33 specifically, the thermal conductivity of the binder, probably have little influence on the thermal  
34 conductivity of the composite, [45] found the opposite. In the present study, the comparison  
35 between C1-H, C2-H and HB-H, which have practically the same dry density, ranging from 410 to 470

1 kg/m<sup>3</sup>, but which showed  $\lambda$  values oscillating between 0.09 and 0.155 W/(m.K), rather tends to the  
 2 conclusion that the binder nature has a significant impact.

3 To conclude, the aforementioned results suggest that density is the parameter that influences the  
 4 most the thermal conductivity. However, the aggregate type was found to have a certain impact, as  
 5 well as the binder type.

6

### 7 3.3. Sorption isotherms

8 Adsorption-desorption isotherms are presented in **Fig. 5** and **Fig. 6**. They are of type II according to  
 9 IUPAC classification [46]. It is consistent with which is commonly observed in literature for bio-based  
 10 materials [47][48] and for composites [49][50].

11  
 12 The comparison of the sorption curves can be made either with the water content expressed in  
 13 kg/m<sup>3</sup> (denoted by  $w$ ) or expressed in kg/kg (denoted by  $u$ ). They are both linked together through  
 14 the dry density of the sample (denoted by  $\rho_d$ ):

15

$$16 \quad w = \rho_d u = \rho_d \left( \frac{m - m_d}{m_d} \right) \quad (2)$$

17

18 where  $m$  is the current mass of the sample and  $m_d$  its dry mass.

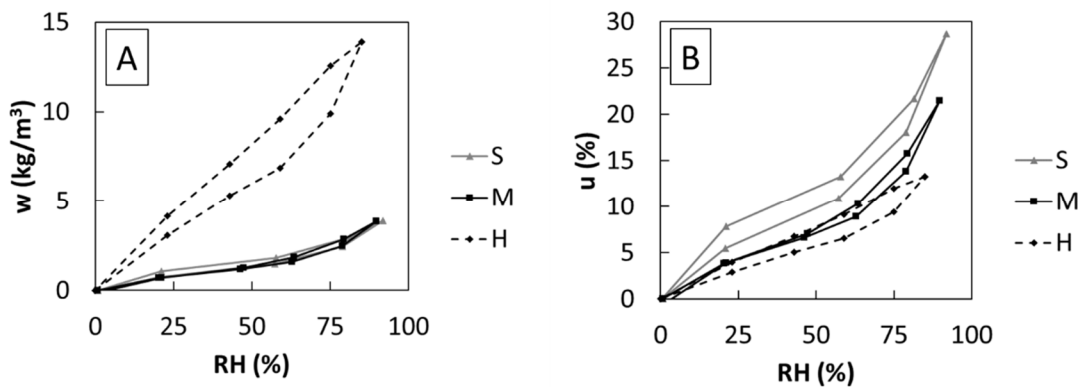
19

20 These two means of comparison do not exactly provide the same information.  $u$  is a specific value. It  
 21 is useful to have the intrinsic curve of a material or a component. For example, to characterize bio-  
 22 based granulates, it is better to use  $u$  than  $w$ . On the other side, the water content in kg/m<sup>3</sup>  
 23 represents the actual water quantity stored in the material volume. This latter should rather be used  
 24 in order to compare the hygroscopic potential of final products, since it is this latter which is involved  
 25 in the mass conservation equations [51]. Let us underline that most of the comparisons in literature  
 26 have been made with water content in kg/kg, which may induce to some ambiguities on the real  
 27 water storage capacity of materials.

28

29 The specific adsorption-desorption curves on the aggregates are shown in **Fig 5B**. The values in kg/m<sup>3</sup>  
 30 reported in the **Fig 5A** correspond to samples of loose aggregates of same apparent density to those  
 31 used to estimate the thermal conductivity, vapor diffusivity and MBV of aggregates. Results are in  
 32 range of what it is generally reported in literature even if moisture content at high hygrometry for  
 33 sunflower pith was greater than that found by [14].

34

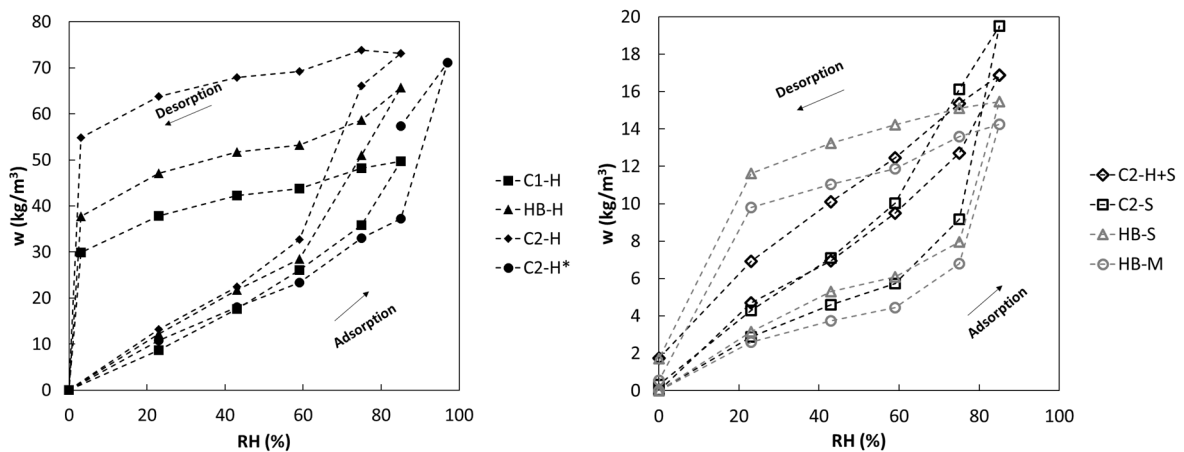


35

1 **Fig. 5.** Adsorption/desorption curves for the three bio-based aggregates with the water content in (A):  
 2  $\text{kg/m}^3$ , and (B):  $\text{kg/kg}$ .

3  
 4 In **Fig 5**, maize and sunflower aggregates exhibited a very similar behavior, with almost no hysteresis.  
 5 On the other side, hemp shiv showed a lower specific water content and a more important, although  
 6 limited, hysteresis. Due to its larger density, the **Fig. 5A** indicates that a volume of loose hemp shiv  
 7 has the ability to store about three times more water than the same volume of loose sunflower or  
 8 maize pith sample.

9 **Fig. 6** shows the adsorption and desorption curves of bio-based composites. The order of magnitude  
 10 obtained for moisture amounts at high hygrometry of composite are in the range of what is  
 11 classically observed for this kind of materials. For example, [14] found for sunflower and maize  
 12 composites a practically identical moisture capacity than the one obtained for HB-S and HB-M, as  
 13 well as the same change in slope at 75% RH. Concerning hemp-based composites, C2-H\*, C2-H, C1-H  
 14 and HB-H give similar behaviors than the ones reported by [52] for sprayed hemp-lime composite,  
 15 and by [53] and [54] for hemp-lime composite. In particular, the strong slope increase in the  
 16 adsorption curve at 80% of RH and the significant hysteresis which can be observed in all the hemp-  
 17 based formulations were also found by numerous authors [48][55][56][57][58].



18  
 19 **Fig. 6.** Adsorption/desorption curves for the eight formulations. Left: hemp-based formulations. Right:  
 20 Pith-based formulations and hemp+pith-based formulation.

21  
 22 The first remark that can be done on the sorption curves of composites is that the tendencies  
 23 observed on the loose aggregates are maintained. Sunflower and maize piths-based formulations  
 24 almost give the same results, with a water content at 80%RH between  $13 \text{ kg/m}^3$  and  $20 \text{ kg/m}^3$ . On  
 25 the other side, all of hemp-based formulations have a stronger water content at 80%RH, that  
 26 oscillates between  $37 \text{ kg/m}^3$  and  $70 \text{ kg/m}^3$ , and show strong hysteresis. These observations are all  
 27 the more surprising that a lower value of water content was found for all the pith-based formulations,  
 28 whatever their density. This first analysis suggests that the sorption curves are more impacted by the  
 29 aggregate than by the binder.

30 Within each group (either pith-based or hemp-based formulations), the influence of the binder can  
 31 however be appreciated, even if it is secondary compared to aggregates' one. Indeed, C binder  
 32 allows a bigger water intake than HB binder, which at the same time allows a bigger water intake  
 33 than C1 binder.

1 All these results indicate dissimilarities between the microstructures of the formulations. In  
 2 particular, [59] suggest that hysteresis in lime composites is due to a double sorption mechanism.  
 3 That is, a fast process that takes place at the surface of the solid and a slow process that consists in  
 4 the integration of the water molecules into the solid matrix. This phenomenon is linked to cellulose  
 5 based materials. The noticeable difference in the hysteretic behavior of hemp-based and pith-based  
 6 composites may be a result of a difference in water exchanges dynamics at the micro-scale.

7 Realistic hygrometry cycles in buildings do not generally exceed 75% of RH and do not fall below 33%  
 8 of RH. Therefore, it is reasonable to focus the study between these two values. Moreover, it seems  
 9 more interesting to compare materials using one single parameter. Moisture capacity, denoted by  $\zeta$ ,  
 10 is the parameter that expresses the capacity of the material to store the water molecules within itself.  
 11 It is calculated as the slope of the adsorption ( $\zeta_{\text{adsorption}}$ ) or desorption ( $\zeta_{\text{desorption}}$ ) isotherms between  
 12 33 and 75% of RH. **Table 5** summarizes the moisture capacity of all isotherm curves.

13  
 14 In the bibliography aforementioned, which only includes adsorption curves, moisture capacity values  
 15 go from 10.44 kg/m<sup>3</sup> [53] to 57.29 kg/m<sup>3</sup> [48], with [56] between both and throwing a value of 26.03  
 16 kg/m<sup>3</sup>. Moisture adsorption capacity of HB-M, HB-S and C2-H\* are in line with these results. Yet, C1-H,  
 17 HB-H and C2-H present a very high capacity of water vapor storage during adsorption comparing to  
 18 other existing materials.

19 A difference between the moisture capacity of adsorption and desorption can be noticed. For hemp-  
 20 bases formulations  $\zeta_{\text{desorption}}$  values are significantly lower than  $\zeta_{\text{adsorption}}$  ones. The same result was  
 21 found by [47]. For pith-based formulations, the difference between  $\zeta_{\text{desorption}}$  and  $\zeta_{\text{adsorption}}$  is within the  
 22 range of uncertainty, and they can thus be considered as equal.

23 In view of these results we can notice that if strong differences exist on  $\zeta_{\text{adsorption}}$  (between 136 kg/m<sup>3</sup>  
 24 and 8 kg/m<sup>3</sup>),  $\zeta_{\text{desorption}}$  remains within a more limited range of values (between 22 kg/m<sup>3</sup> and 5 kg/m<sup>3</sup>).  
 25 The distinction that was observed on the sorption curves in function of the aggregate nature is  
 26 clearly visible on  $\zeta_{\text{adsorption}}$ , but it is no more visible if the comparison is made on  $\zeta_{\text{desorption}}$ . For this latter,  
 27 the distinction is rather between low density formulations, which have  $\zeta_{\text{desorption}}$  values bellow  
 28 10 kg/m<sup>3</sup> and high density formulations which rather shows values between 16 kg/m<sup>3</sup> and 22 kg/m<sup>3</sup>  
 29 (excepting values of C2-H).

**Table 5** Summary of the hygric properties.

Type of samples	$\zeta_{\text{adsorption}}$ (kg/m <sup>3</sup> )	$\zeta_{\text{desorption}}$ (kg/m <sup>3</sup> )	$\mu$ (-)	MBV <sub>practical</sub> (g/m <sup>2</sup> /%RH)	$\zeta_{\text{ideal}}$ (kg/m <sup>3</sup> )	$\rho_{\text{aggregate}}^*$ (kg/m <sup>3</sup> )	$\zeta_{\text{aggregate}}^*$ (kg/m <sup>3</sup> )
C2-S	12 ±NA	15 ±NA	7 ±1.4	1.21 ±NA	6.7	0.05	23
C2-H	136 ±NA	8 ±NA	3.4 ±0.1	1.98±0.09	8.9	-	-
C2-H*	47 ±NA	20 ±NA	3.9 ±0.2	1.63 ±NA	6.7	0.15	10
C2-H+S	15 ±3	16 ±0.4	3.9 ±0.6	1.71 ±NA	7.4	H: 0.08 ; S: 0.03	15
HB-S	8 ±0.4	5 ±0.05	4.7±0.3	1.25 ±0.06	5.0	0.05	16
HB-M	10 ±0.5	7 ±0.5	5.1 ±0.6	1.35 ±0.03	5.7	0.04	13
C1-H	57 ±NA	18 ±NA	4.2 ±0.7	1.56 ±0.05	6.6	0.12	5
HB-H	92 ±NA	22 ±NA	4.0 ±0.3	1.60 ±0.07	6.7	0.11	5
Hemp shiv (H)	14 ±0.4	17 ±0.2	1.2 ±0.002	2.90 ±0.02	6.6	-	-
Sunflower pith (S)	3 ±0.2	3 ±0.1	1.0 ±0.006	2.60 ±0.03	4.4	-	-

31



### 1 3.4. Water vapor permeability

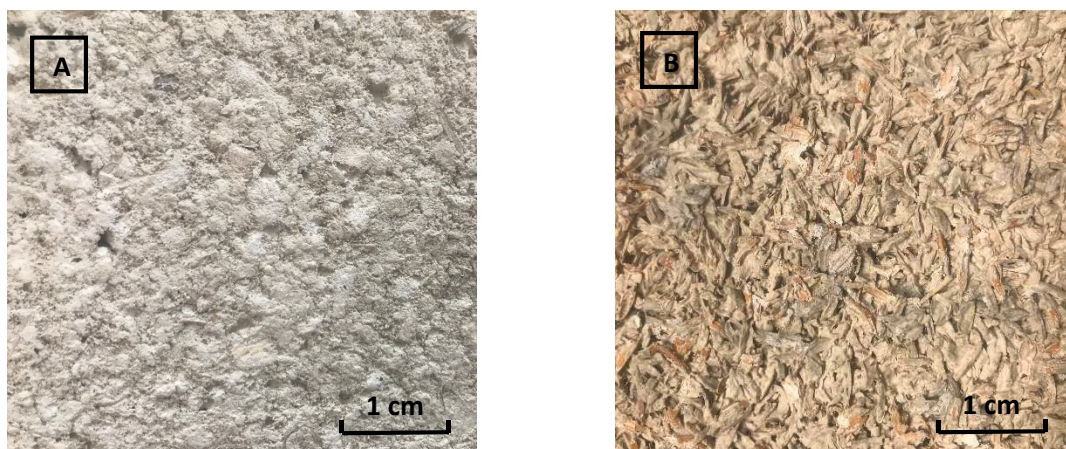
2 Wet cup test results are presented in the **Table 5** in terms of  $\mu$  value, which is the resistance to  
3 diffusion of vapor within the material.  $\mu$  value of loose aggregates was found to be close to 1. It  
4 means that, once the permanent state is reached, these latter have almost no impact on the vapor  
5 diffusion.

6  
7 Composites present values between 3.4 and 4.9, except for C2-S, whose value is 7. These values are  
8 much lower than those observed by [10][12][48][55] and [57], which range from 5 to 12 for hemp,  
9 rape straw and flax composites. This difference with the literature is probably attributable to  
10 experimental conditions, which could have a significant impact on the values obtained. With the cup  
11 method, [60] studied the influence of different test parameters such as thickness and area of the  
12 specimen, thickness of the air gap at the lower surface of the specimen, air velocity, cup height, and  
13 hygrometry inside and outside the cup. Especially for hygroscopic materials such as bio-aggregate  
14 based building materials, the water vapor permeability is strongly linked to the local relative  
15 humidity. Thus, measurements of water vapor permeability, which are performed at different levels  
16 of relative humidity (dry-cup and wet-cup), may result in different values for one saline solution and  
17 the same material. The increase of the water vapor permeability with relative humidity was proved  
18 by [52] and [55]: the water vapor permeability diffusion coefficient increased by a factor of seven  
19 depending on the hygrometry. This may have been due to contribution of liquid water transport  
20 through the sample, which becomes noticeable at higher humidity values.

21  
22 It is commonly assumed that, other parameters being equal,  $\mu$  should increase with density (and thus  
23 decrease with porosity), which is consistent with the results obtained with the formulation C2-H and  
24 C2-H\*. An increase of density from 1440 kg/m<sup>3</sup> to 1600 kg/m<sup>3</sup> led to an increase of  $\mu$  from 3.4 to 3.9.  
25 This tendency is however no more observed when the binder-aggregate couple is changed.

26 More precisely, pith-based formulations show globally higher values of  $\mu$ . The one of the formulation  
27 C2-S is twice that of C2-H\* and C2-S+H, while their binder and their density are approximatively the  
28 same. In the same line, the  $\mu$ -values of formulations HB-S and HB-M are in the same range as those  
29 of the hemp-based formulations, while their density is strongly lower. Actually, as it was already  
30 mentioned for the thermal conductivity measurements, morphology of hemp-based and pith-based  
31 composites are clearly different. As it is sketched in the pictures of the **Fig 7**, while open connected  
32 pores are obviously visible at the surface of the former, the latter exhibit a flatter surface with almost  
33 no asperity. Even if no direct link can be established between this visual observation and connectivity  
34 of samples' porous network, it clearly indicates a difference in microstructure between these two  
35 formulations.

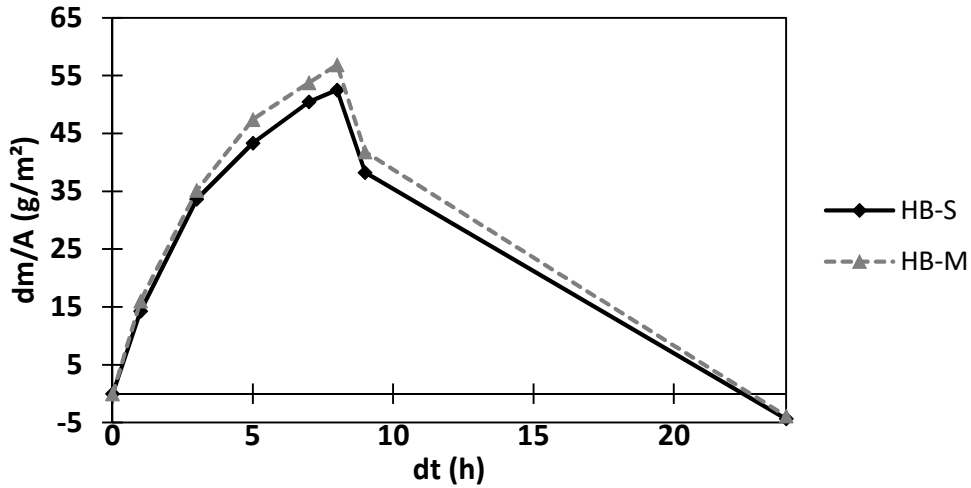
36



1 **Fig. 7.** Pictures of the surface texture of (A) pith-based formulations and (B) hemp-based  
 2 formulations.  
 3  
 4

5 **4. Discussion on the hygroscopic potential of pith-based composites**

6 The moisture buffering value of aggregates and composites has been estimated following the  
 7 NordTest protocol [33]. Results are show in **Table 5**. An example of the mass tracking curve, from  
 8 which  $MBV_{practical}$  is determined, of HB-S and HB-M is given in **Fig. 8**.



9  
 10 **Fig. 8.** Mass tracking of HB-S and HB-M during the MBV test.

11 The first remark that can be made is that the results can be divided in three groups. Loose aggregates  
 12 have a moisture buffering value (MBV) higher than  $2 \text{ g/m}^2/\%RH$ , which makes them materials with an  
 13 excellent hygroscopic potential according to the classification proposed by [33]. The hemp-based and  
 14 hemp+pith-based formulations have values ranging between  $1.56 \text{ g/m}^2/\%RH$  and  $1.71 \text{ g/m}^2/\%RH$ .  
 15 Finally, the MBV of the pith-based formulations is rather between  $1.21 \text{ g/m}^2/\%RH$  and  
 16  $1.35 \text{ g/m}^2/\%RH$ . All these formulations can be classified as materials with a good hygroscopic  
 17 potential.

18 This hierarchy on the hygroscopic potential is quite expected with regard to the results of both  
 19 sorption and vapor diffusion properties of the tested materials. However, in view of the significant  
 20 dissimilarities found on the sorption curves, a wider range of MBV may have been anticipated.

21 Actually, the storage capacity  $\zeta$  is known to significantly influence the hygroscopic potential of  
 22 materials [61]. However, as it is sketched in the results of the section 3.4, high uncertainty exists on  
 23 this value since more than one order of magnitude of difference can be observed in some samples  
 24 between the storage capacity in adsorption and in desorption.

25 [33] have developed an analytical solution in order to predict the MBV value in function of  $\zeta$  and  $\mu$ .  
 26 The calculated value is called the  $MBV_{ideal}$ , while we recall that the measured one is denoted by  
 27  $MBV_{practical}$ . Another way to use this analytical solution can be to calculate what would be the storage  
 28 capacity that would effectively lead to an  $MBV_{ideal}$  equal to the  $MBV_{practical}$ . This storage capacity will  
 29 be noted  $\zeta_{ideal}$  throughout the rest of this paper. At  $23^\circ C$ , the vapor pressure at saturation and the  
 30 free vapor diffusion coefficient in air are respectively equal to  $2814 \text{ Pa}$  and  $1.97 \cdot 10^{-10} \text{ kg}/(\text{m}\cdot\text{s}\cdot\text{Pa})$ . By  
 31 application of the  $MBV_{ideal}$ 's formula with  $MBV_{ideal} = MBV_{practical}$  and cycles duration of 24 hours, it  
 32 leads to:  
 33

34 
$$\zeta_{ideal} \approx 0.65 \mu (MBV_{practical})^2 \quad (3)$$
  
 35

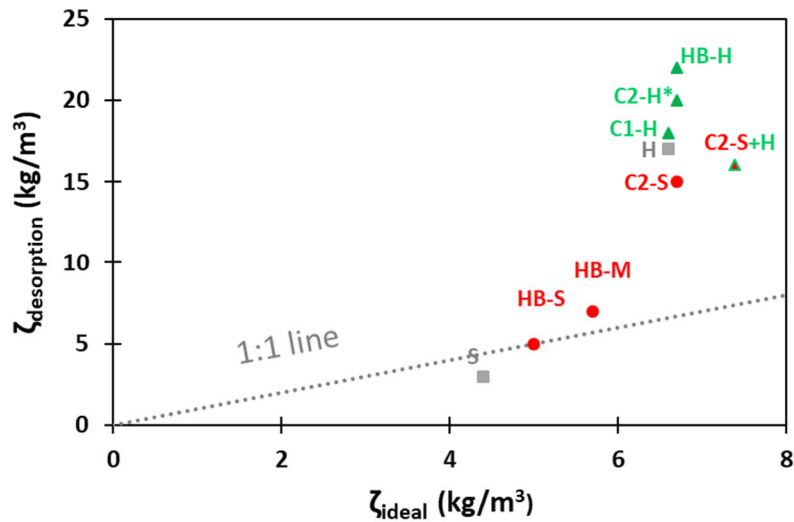
1 In this relation  $MBV_{practical}$  must be expressed in  $g/(m^2.\%RH)$ , while  $\zeta_{ideal}$  is in  $kg/m^3$ .

2

3 The obtained values are reported in the **Table 5**. The first remark that can be made is that for most of  
 4 the formulations, both  $\zeta_{desorption}$  and  $\zeta_{adsorption}$  values (cf. **Table 4**) are above  $\zeta_{ideal}$  ones. However  
 5 while  $\zeta_{desorption}$  remains in the same order of magnitude than  $\zeta_{ideal}$ ,  $\zeta_{adsorption}$  values appear to be  
 6 strongly higher. The same kind of results were found by [47] on hemp composite. It led to the  
 7 recommendation to rather use cycles of relative humidity (or at least the desorption curves) than the  
 8 adsorption curves to predict the hygroscopic potential of hemp composites. One reason of that could  
 9 be that not all the water within the material is mobilized during the cycles of relative humidity. Thus,  
 10 if the adsorption curve starts on a strongly dried material, some of the water that will be captured  
 11 within the material microstructure will not be released during the desorption stage, unless it is  
 12 subjected to severe drying conditions, that would not classically happen.

13

14 Interestingly, as it is sketched in the **Fig. 9**,  $\zeta_{desorption}$  and  $\zeta_{ideal}$  appear to be almost the same for  
 15 loose sunflower pith and lighter formulations (HB-S and HB-M), while more important differences are  
 16 observed for loose hemp shiv and denser formulations. It tends to indicate, that static characteristics  
 17 (namely  $\zeta_{desorption}$  and  $\mu$ ) are not sufficient to accurately reproduce dynamic hygroscopic behavior  
 18 of hemp shiv and dense formulations of this study. This difference between static and dynamic  
 19 hygroscopic characteristics has already been highlighted by [62]. To avoid this problem, the efficiency  
 20 of the aggregates within composites will be studied through the  $\zeta_{ideal}$  values, since they are the ones  
 21 which are linked to the dynamic behavior of the material.



22

23 **Fig. 9.** Adsorption coefficient estimated from the desorption curve in function of the one calculated  
 24 from  $MBV_{practical}$  through the eq. (3).

25

26

27 Mass proportions of the aggregates in mixtures, denoted by  $p_{aggregate}$ , are indicated in the **Table 1**.

28 From this value, it is possible to know the mass of aggregate per unit of composite samples volume,

29 denoted by  $\rho_{aggregate}^*$ , through the relation:

30

$$31 \rho_{aggregate}^* = \frac{m_{wet}}{V} p_{aggregate} \quad (4)$$

32

33 where  $m_{wet}$  is the mass of the composite sample just after mixing, while  $V$  is its volume. Values of

34  $\rho_{aggregate}^*$  obtained for the different formulations are reported in the **Table 5**. For hemp-based

35 formulations,  $\rho_{aggregate}^*$  remains quite close to the loose density of hemp shiv (between  $110 kg/m^3$

1 and 150 kg/m<sup>3</sup> for the former and 100 kg/m<sup>3</sup> for the latter). It indicates that the binder has filled the  
2 gaps between hemp particles without significantly modifying their geometrical arrangement. On the  
3 opposite,  $\rho_{\text{aggregate}}^*$  of pith-based formulations are about four times higher than loose density of  
4 sunflower pith (between 40 kg/m<sup>3</sup> and 50 kg/m<sup>3</sup> for the former and 14 for the latter). In consequence,  
5 this probably indicates a compaction of the pith particles during manufacturing of the samples, the  
6 pith is a rather soft material that can be easily compressed, compared to the harder hemp shiv.

7  
8 The ideal storage capacities of the aggregates (either hemp shiv or sunflower pith) which are  
9 calculated with the eq. (5) and whose values are reported in the **Table 5**, will be noted  $\zeta_{\text{aggregate}}^{\text{ideal}}$ .  
10 They can be understood as the dynamic storage capacity of loose aggregate samples. For a given  
11 aggregate microstructure, it should vary linearly with apparent density. In consequence, if aggregates  
12 are not subjected to any microstructure modification nor interaction with the binder, their  
13 contribution to the dynamic storage capacity of the composite will be equal to:

$$\zeta_{\text{aggregate}}^* = \frac{\rho_{\text{aggregate}}^*}{\rho_{\text{aggregate}}} \zeta_{\text{aggregate}}^{\text{ideal}} \quad (5)$$

16  
17  $\zeta_{\text{aggregate}}^*$  has been calculated for all the formulations and the results are shown in the **Table 5**. For  
18 hemp-based formulations,  $\zeta_{\text{aggregate}}^*$  is very close to the dynamic storage capacity of the composite  
19 (that is the  $\zeta_{\text{ideal}}$  of the composite). It denotes that hemp shiv aggregates play the main role in the  
20 dynamic hygroscopic behavior of these formulations and that the binder does not alter significantly  
21 their hygroscopic potential. On the opposite,  $\zeta_{\text{aggregate}}^*$  values are clearly higher than  $\zeta_{\text{ideal}}$  ones for  
22 pith-based formulations. This observation is another proof of the strong interaction between the  
23 binder and the pith, that alters their hygroscopic potential. It is consistent with the differences in  
24 behavior which were observed for pith-based formulations for both thermal conductivity and vapor  
25 diffusivity. All these results converge to the fact that when they are mixed with the binder, sunflower  
26 and maize pith aggregates undergo quite important microstructural transformations, which limit  
27 their contribution to both thermal insulation and moisture buffering potential.

28 In consequence, one challenge for the optimized use of this kind of aggregate might be the  
29 development of dedicated binders which would limit these interactions while keeping acceptable  
30 mechanical strength.

31 Anyway, despite this observation, mechanical, thermal and hygroscopic performance of the tested  
32 pith-based composites remain quite close to hemp-composite ones. In addition, this kind of  
33 granulate was found to allow the fabrication of low-density insulation composite with a quite  
34 competitive thermal conductivity and hygroscopic performances. Thus, even if more researches need  
35 to be conducted in order to optimize their use, pith aggregates appear to be particularly promising.

## 36 **5. Conclusion**

37 Bio-based building materials, namely vegetal composites, are very promising for modern  
38 construction since they are eco-responsible due to their lower embodied energy and to the  
39 possibility of local production. The current challenge is to determine the formulations that present  
40 interesting mechanical and hygrothermal qualities while respecting environmental and economic  
41 criteria. Numerous pieces of research work have studied hemp composites in the last few years, but  
42 other aggregates such as sunflower and maize pith are little known. The interest of studying new  
43 aggregates is to propose greater geographical availability of resources and this way reduce the  
44 carbon print linked to transportation.

1 In this paper, vegetal composites made with three kinds of binder mixed with hemp shiv, sunflower  
2 pith, are/or maze pith are studied. Even if these bio-based composites cannot be used in load-  
3 bearing members of the building, some of them qualify to be used as plaster, as a wall, as floor or as  
4 a roof according to French hemp construction guide (HB-H, C2-H+S and C2-S) whereas others qualify  
5 as roof material (HB-S and HB-M). This proves that pith composites can have the same applications as  
6 hemp composites. The mechanical resistance of vegetal composites has been found to be  
7 proportional to density, as well as thermal conductivity. Moreover, it has been observed that  
8 thermal conductivity is also influenced more moderately by the type of aggregates and the type of  
9 binder.

10 In this study, some composites show remarkable hygrothermal characteristics, particularly those  
11 based on hemp shiv (C2-H, C1-H and HB-H). Thus we can conclude that the type of aggregate has a  
12 considerable impact on these properties. Hysteresis is present for all the formulations as it is  
13 commonly observed in bio-based materials. The study of the MBV is more accurate when calculated  
14 from the cycles of RH rather than from the sorption curves, given that the cycles represent more  
15 closely the dynamic behavior.

16 For all the aforementioned properties, it has been noticed that in most cases, the behavior of the  
17 materials cannot be properly explained by the aggregate type or the binder type. On the contrary,  
18 interactions between binder and aggregate has been observed, namely chemical interactions, a  
19 transformation of microstructure and the immersion and isolation of aggregate particles. The latter  
20 two seem to be stronger underlined for pith composites.

21 To conclude, pith composites studied in this paper met mechanical and hygrothermal requirements  
22 expected for insulating bio-based materials. However, possibly due to the interactions between the  
23 binder and pith particles, the hygrothermal potential of these latter within the composite seemed to  
24 be lowered. This result suggests that it should be interesting to search for dedicated binders for pith  
25 aggregates that enhance the hygroscopic and mechanical properties of the composite.

## 26 **Aknowledgements**

27 Authors would like thank the financial support from the Agence de la transition écologique (ADEME),  
28 France.

## 29 **References**

- 30 [1] U. E. I. Administration, “International Energy Outlook 2017 Overview,” 2017.
- 31 [2] European Comission, “Energy datasheets: EU27 countries,” 2020. [Online]. Available:  
32 [https://ec.europa.eu/energy/sites/ener/files/energy\\_statistical\\_countrydata\\_sheets.xlsx](https://ec.europa.eu/energy/sites/ener/files/energy_statistical_countrydata_sheets.xlsx).  
33 [Accessed: 01-May-2020].
- 34 [3] UN Environment and International Energy Agency, “Global Status Report 2017,” 2017.
- 35 [4] J. C. Morel, A. Mesbah, M. Oggero, and P. Walker, “Building houses with local  
36 materials: Means to drastically reduce the environmental impact of construction,” *Build.*  
37 *Environ.*, vol. 36, no. 10, pp. 1119–1126, 2001.
- 38 [5] Association construire en chanvre and Fédération Française du Bâtiment, *Construire en*  
39 *chanvre - règles professionnelles d'exécution*, 2ème édit. Fédération Française du  
40 Bâtiment, 2009.
- 41 [6] RFCP (ouvrage collectif), *Règles Professionnelles de la construction en paille*. 2011.
- 42 [7] M. Viel, F. Collet, and C. Lanos, “Chemical and multi-physical characterization of

- 1 agro-resources' by-product as a possible raw building material," *Ind. Crops Prod.*, vol.  
2 120, no. May, pp. 214–237, 2018.
- 3 [8] M. Amziane, Sofiane; Sonebi, "Overview on biobased building material made with  
4 plant aggregate," *Sustain. Constr. Mater. Technol.*, no. June, 2016.
- 5 [9] C. Magniont, "Contribution à la formulation et à la caractérisation d'un écomatériau de  
6 construction à base d'agroressources," 2010.
- 7 [10] R. Walker, S. Pavia, and R. Mitchell, "Mechanical properties and durability of hemp-  
8 lime concretes," *Constr. Build. Mater.*, vol. 61, pp. 340–348, 2014.
- 9 [11] P. De Bruijn and P. Johansson, "Moisture fixation and thermal properties of lime-hemp  
10 concrete," *Constr. Build. Mater.*, vol. 47, pp. 1235–1242, 2013.
- 11 [12] A. Evrard, "Transient hygrothermal behavior of Lime-Hemp Materials," Ecole  
12 Polytechnique de Louvain, 2008.
- 13 [13] T. M. Dinh, C. Magniont, M. Coutand, and G. Escadeillas, "Hemp concrete using  
14 innovative pozzolanic binder," in *First International Conference on Bio-based  
15 Building Materials*, 2015, no. June 2015.
- 16 [14] M. Lagouin, C. Magniont, P. Sénéchal, P. Moonen, J. E. Aubert, and A. Laborel-  
17 préneron, "Influence of types of binder and plant aggregates on hygrothermal and  
18 mechanical properties of vegetal concretes," *Constr. Build. Mater.*, vol. 222, pp. 852–  
19 871, 2019.
- 20 [15] M. R. Ahmad, B. Chen, S. Yousefi Oderji, and M. Mohsan, "Development of a new  
21 bio-composite for building insulation and structural purpose using corn stalk and  
22 magnesium phosphate cement," *Energy Build.*, vol. 173, pp. 719–733, 2018.
- 23 [16] F. Collet and S. Pretot, "Thermal conductivity of hemp concretes: Variation with  
24 formulation, density and water content," *Constr. Build. Mater.*, vol. 65, pp. 612–619,  
25 2014.
- 26 [17] C. Gross and P. Walker, "Racking performance of timber studwork and hemp-lime  
27 walling," *Constr. Build. Mater.*, vol. 66, pp. 429–435, 2014.
- 28 [18] V. Cérézo, "Propriétés mécaniques , thermiques et acoustiques d ' un matériau à base  
29 de particules végétales : approche expérimentale et modélisation théorique," ENTPE,  
30 2005.
- 31 [19] T. T. Nguyen, "Contribution à l ' étude de la formulation et du procédé de fabrication  
32 d ' éléments de construction en béton de chanvre," Université de Bretagne Sud, 2010.
- 33 [20] R. Hanley and S. Pavía, "A study of the workability of natural hydraulic lime mortars  
34 and its influence on strength," *Mater. Struct. Constr.*, vol. 41, no. 2, pp. 373–381, 2008.
- 35 [21] F. Murphy, S. Pavia, and R. Walker, "An assessment of the physical properties of lime-  
36 hemp concrete," in *BRI/CRI*, 2010, vol. 2, pp. 431–439.
- 37 [22] Y. Wei, C. Song, B. Chen, and M. R. Ahmad, "Experimental investigation on two new  
38 corn stalk biocomposites based on magnesium phosphate cement and ordinary Portland  
39 cement," *Constr. Build. Mater.*, vol. 224, pp. 700–710, 2019.
- 40 [23] V. Nozahic and S. Amziane, "Composites : Part A Influence of sunflower aggregates  
41 surface treatments on physical properties and adhesion with a mineral binder," *Compos.  
42 PART A*, vol. 43, no. 11, pp. 1837–1849, 2012.
- 43 [24] L. Arnaud, C. Véronique, and S. Driss, "Global approach for the design of building  
44 material containing lime and vegetable particles," in *The sixth International Symposium*

- 1            *of Cement and Concrete*, 2006, pp. 1261–1265.
- 2 [25] T.-T. Nguyen, V. Picandet, S. Amziane, and C. Baley, “Influence of compactness and  
3 hemp hurd characteristics on the mechanical properties of lime and hemp concrete,”  
4 *Rev. Eur. génie Civ.*, vol. 13, no. 9, pp. 1039–1050, 2009.
- 5 [26] T. T. Nguyen, V. Picandet, P. Carre, T. Lecompte, S. Amziane, and C. Baley, “Effect  
6 of compaction on mechanical and thermal properties of hemp concrete,” *Eur. J.*  
7 *Environ. Civ. Eng.*, vol. 14, no. 5, pp. 545–560, 2010.
- 8 [27] A. Bourdot, C. Magniont, M. Lagouin, C. Niyigena, P. Evon, and S. Amziane, “Impact  
9 of bio-aggregates properties on the chemical interactions with mineral binder,  
10 application to vegetal concrete,” *J. Adv. Concr. Technol.*, vol. 17, pp. 542–558, 2019.
- 11 [28] M. Palumbo, “Contribution to the development of new bio-based thermal insulation  
12 materials made from vegetal pith and natural binders : hygrothermal performance , fire  
13 reaction and mould growth resistance,” 2015.
- 14 [29] Y. Brouard, N. Belayachi, D. Hoxha, N. Ranganathan, and S. Méo, “Mechanical and  
15 hygrothermal behavior of clay – Sunflower ( *Helianthus annuus* ) and rape straw  
16 ( *Brassica napus* ) plaster bio-composites for building insulation,” *Constr. Build.*  
17 *Mater.*, vol. 161, pp. 196–207, 2018.
- 18 [30] J. D. Mathias *et al.*, “Upcycling sunflower stems as natural fibers for biocomposite  
19 applications,” *BioResources*, 2015. .
- 20 [31] A. Laborel-Préneron, C. Magniont, and J. E. Aubert, “Hygrothermal properties of  
21 unfired earth bricks: Effect of barley straw, hemp shiv and corn cob addition,” *Energy*  
22 *Build.*, vol. 178, pp. 265–278, 2018.
- 23 [32] M. S. Abbas, F. McGregor, A. Fabbri, and Y. Ferroukhi, “Influence of origin and year  
24 of harvest on the performance of pith mortars,” in *3rd International Conference of Bio-*  
25 *Based Building Materials*, 2019.
- 26 [33] C. Rode *et al.*, “Moisture Buffering of Building Materials,” *BYG Rep.*, vol. R-127,  
27 2005.
- 28 [34] S. Amziane, F. Collet, M. Lawrence, C. Magniont, V. Picandet, and M. Sonebi,  
29 “Recommendation of the RILEM TC 236-BBM: characterisation testing of hemp shiv  
30 to determine the initial water content, water absorption, dry density, particle size  
31 distribution and thermal conductivity,” *Mater. Struct. Constr.*, vol. 50, no. 3, 2017.
- 32 [35] I. Ceyte, “Béton de chanvre, définition des caractéristiques mécaniques de la  
33 chènevotte, Travail de Fin d’Études.,” 2008.
- 34 [36] E. Gourlay and L. Arnaud, “Des matières premières au béton de chanvre : optimisation  
35 des propriétés thermiques et mécaniques,” in *20ème congrès français de Mécanique*,  
36 2011, pp. 1–6.
- 37 [37] S. Kioy, “Lime-hemp composites: compressive strenght and resistance to fungal  
38 attacks. MEng dissertation, recalled in Appendix 1: Resistance to compression and  
39 stress-strain properties,” 2013.
- 40 [38] P. Tronet, T. Lecompte, V. Picandet, and C. Baley, “Study of lime hemp concrete  
41 (LHC) - Mix design, casting process and mechanical behaviour,” *Cem. Concr.*  
42 *Compos.*, vol. 67, pp. 60–72, 2016.
- 43 [39] A. Fabbri, F. Mcgregor, I. Costa, and P. Faria, “Effect of temperature on the sorption  
44 curves of earthen materials,” *Mater. Struct.*, vol. 50, no. 6, pp. 1–13, 2017.



- 1 [40] F. Collet, M. Bart, L. Serres, and J. Miriel, "Porous structure and water vapour sorption  
2 of hemp-based materials," *Constr. Build. Mater.*, vol. 22, no. 6, pp. 1271–1280, 2008.
- 3 [41] F. McGregor, A. Heath, E. Fodde, and A. Shea, "Conditions affecting the moisture  
4 buffering measurement performed on compressed earth blocks," *Build. Environ.*, vol.  
5 75, pp. 11–18, 2014.
- 6 [42] K. Svennberg, "Moisture Buffering in the Indoor Environment. Report TVBH-1016  
7 Lund 2006 Building Physics LTH," 2006.
- 8 [43] F. McGregor, A. Fabbri, J. Ferreira, T. Simões, P. Faria, and J. C. Morel, "Procedure to  
9 determine the impact of the surface film resistance on the hygric properties of  
10 composite clay/fibre plasters," *Mater. Struct. Constr.*, vol. 50, no. 4, 2017.
- 11 [44] R. Walker and S. Pavía, "Moisture transfer and thermal properties of hemp – lime  
12 concretes," *Constr. Build. Mater.*, vol. 64, pp. 270–276, 2014.
- 13 [45] E. Gourlay and L. Arnaud, "Comportement hygrothermique des murs de béton de  
14 chanvre," *Proc. Actes du congrès SFT , Le Touquet Fr.*, vol. 3237, no. February, 2010.
- 15 [46] D. H. Everett, "Reporting data on adsorption from solution at the SOLid/SOLution  
16 interface (Recommendations 1986)," *Pure Appl. Chem.*, vol. 58, no. 7, pp. 967–984,  
17 1986.
- 18 [47] A. Fabbri and F. McGregor, "Impact of the determination of the sorption-desorption  
19 curves on the prediction of the hemp concrete hygrothermal behaviour," *Constr. Build.  
20 Mater.*, vol. 157, pp. 108–116, 2017.
- 21 [48] M. Rahim *et al.*, "Characterization of flax lime and hemp lime concretes: Hygric  
22 properties and moisture buffer capacity," *Energy Build.*, vol. 88, pp. 91–99, 2015.
- 23 [49] H. Derluyn, D. Derome, J. Carmeliet, E. Stora, and R. Barbarulo, "Hysteretic moisture  
24 behavior of concrete: Modeling and analysis," *Cem. Concr. Res.*, vol. 42, no. 10, pp.  
25 1379–1388, 2012.
- 26 [50] V. Baroghel-Bouny, "Water vapour sorption experiments on hardened cementitious  
27 materials. Part I: Essential tool for analysis of hygral behaviour and its relation to pore  
28 structure," *Cem. Concr. Res.*, vol. 37, no. 3, pp. 414–437, 2007.
- 29 [51] M. Y. Ferroukhi, K. Abahri, R. Belarbi, K. Limam, and A. Nouviaire, "Experimental  
30 validation of coupled heat , air and moisture transfer modeling in multilayer building  
31 components," *Heat Mass Transf.*, no. December, 2015.
- 32 [52] J. Chamoin, "Optimisation des propriétés (physiques, mécaniques et hydriques) de  
33 bétons de chanvre par la maîtrise de la formulation," INSA de Rennes, 2013.
- 34 [53] E. Latif, M. Lawrence, A. Shea, and P. Walker, "Moisture buffer potential of  
35 experimental wall assemblies incorporating formulated hemp-lime," *Build. Environ.*,  
36 vol. 93, no. P2, pp. 199–209, 2015.
- 37 [54] P. De Bruijn and P. Johansson, "Moisture fixation and thermal properties of lime-hemp  
38 concrete," *Constr. Build. Mater.*, vol. 47, pp. 1235–1242, 2013.
- 39 [55] F. Collet, J. Chamoin, S. Pretot, and C. Lanos, "Comparison of the hygric behaviour of  
40 three hemp concretes," *Energy Build.*, vol. 62, pp. 294–303, 2013.
- 41 [56] B. Mazhoud, F. Collet, S. Pretot, and J. Chamoin, "Hygric and thermal properties of  
42 hemp-lime plasters," *Build. Environ.*, vol. 96, pp. 206–216, 2016.
- 43 [57] M. Rahim, O. Douzane, A. D. Tran Le, G. Promis, and T. Langlet, "Characterization  
44 and comparison of hygric properties of rape straw concrete and hemp concrete," *Constr.*

- 1 *Build. Mater.*, vol. 102, pp. 679–687, 2016.
- 2 [58] Y. Aït Oumeziane, M. Bart, S. Moissette, and C. Lanos, “Modélisation du transfert  
3 d’air, de masse et de chaleur aux travers de parois multicouches,” in *Xème Colloque*  
4 *Interuniversitaire Franco-Québécois sur la Thermique des Systèmes*, 2011.
- 5 [59] B. Seng, C. Magniont, and S. Lorente, “Characterization of a precast hemp concrete .  
6 Part I: Physical and thermal properties,” *J. Build. Eng.*, vol. 24, no. July 2018, p.  
7 100540, 2019.
- 8 [60] O. Vololonirina, M. Coutand, and B. Perrin, “Characterization of hygrothermal  
9 properties of wood-based products - Impact of moisture content and temperature,”  
10 *Constr. Build. Mater.*, vol. 63, pp. 223–233, 2014.
- 11 [61] F. McGregor, A. Heath, A. Shea, and M. Lawrence, “The moisture buffering capacity  
12 of unfired clay masonry,” *Build. Environ.*, vol. 82, pp. 599–607, 2014.
- 13 [62] S. Dubois, F. McGregor, F. Lebeau, A. Evrard, and A. Heath, “An inverse modelling  
14 approach to estimate the hygric parameters of clay-based masonry during a moisture  
15 buffer value test,” *Build. Environ.*, vol. 81, pp. 192–203, 2014.

16